

Large magnetocaloric effect of $\text{Ho}_x\text{Er}_{1-x}\text{Ni}$ ($0 \leq x \leq 1$) compounds

X. Q. Zheng, B. Zhang, H. Wu, F. X. Hu, Q. Z. Huang, and B. G. Shen

Citation: *Journal of Applied Physics* **120**, 163907 (2016); doi: 10.1063/1.4966655

View online: <http://dx.doi.org/10.1063/1.4966655>

View Table of Contents: <http://scitation.aip.org/content/aip/journal/jap/120/16?ver=pdfcov>

Published by the [AIP Publishing](#)

Articles you may be interested in

[Magnetic properties and magnetocaloric effects of \$\text{Gd}_x\text{Er}_{1-x}\text{Ga}\$ \(\$0 \leq x \leq 1\$ \) compounds](#)

J. Appl. Phys. **115**, 17A905 (2014); 10.1063/1.4854875

[Large reversible magnetocaloric effects in \$\text{ErFeSi}\$ compound under low magnetic field change around liquid hydrogen temperature](#)

Appl. Phys. Lett. **102**, 092401 (2013); 10.1063/1.4794415

[Tunable spin reorientation transition and magnetocaloric effect in \$\text{Sm}_{0.7-x}\text{La}_x\text{Sr}_{0.3}\text{MnO}_3\$ series](#)

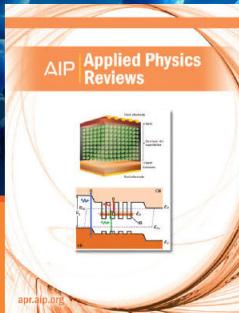
J. Appl. Phys. **113**, 013911 (2013); 10.1063/1.4773337

[Magnetic properties and magnetocaloric effects in \$\text{R}_3\text{Ni}_2\$ \(\$\text{R}=\text{Ho}\$ and \$\text{Er}\$ \) compounds](#)

Appl. Phys. Lett. **99**, 132504 (2011); 10.1063/1.3643142

[Magnetocaloric effects in \$\text{RNiIn}\$ \(\$\text{R}=\text{Gd}-\text{Er}\$ \) intermetallic compounds](#)

J. Appl. Phys. **109**, 123926 (2011); 10.1063/1.3603044



NEW Special Topic Sections

NOW ONLINE
Lithium Niobate Properties and Applications:
Reviews of Emerging Trends

AIP | Applied Physics Reviews

Large magnetocaloric effect of $\text{Ho}_x\text{Er}_{1-x}\text{Ni}$ ($0 \leq x \leq 1$) compounds

X. Q. Zheng,^{1,a)} B. Zhang,² H. Wu,³ F. X. Hu,² Q. Z. Huang,³ and B. G. Shen^{2,a)}

¹*School of Materials Science and Engineering, University of Science and Technology Beijing, Beijing 100083, People's Republic of China*

²*State Key Laboratory for Magnetism, Institute of Physics, Chinese Academy of Sciences, Beijing 100190, People's Republic of China*

³*NIST Center for Neutron Research, National Institute of Standards and Technology, Gaithersburg, Maryland 20899, USA*

(Received 4 August 2016; accepted 18 October 2016; published online 28 October 2016)

A secondary magnetic transition (spin reorientation transition) below Curie temperature in ErNi was observed via different characterization techniques. Ho-substitution for Er atoms has a great impact on the magnetic property and magnetocaloric effect. The two magnetic transitions change close to each other with 10% of Ho-substitution at the Er site. It is also found that 10% of Ho-substitution contributes up to $\sim 14.9\%$ of enhancement on the maximal magnetic entropy change (ΔS_M) and $\sim 21.9\%$ of enhancement on the maximal adiabatic temperature change (ΔT_{ad}). The maximum value of ΔS_M and ΔT_{ad} for $\text{Ho}_{0.1}\text{Er}_{0.9}\text{Ni}$ compound is as high as 34 J/kg K and 8.9 K, respectively, under a field change of 0–5 T. The relationship between the maximal ΔS_M and the refrigerant temperature width (δT_{FWHM}) for $\text{Ho}_x\text{Er}_{1-x}\text{Ni}$ ($0 \leq x \leq 1$) compounds is analyzed. The enhancement of MCE for $\text{Ho}_{0.1}\text{Er}_{0.9}\text{Ni}$ compound is considered to be resulted from the tendency of merging of spin reorientation transition and ferromagnetic to paramagnetic transition. Published by AIP Publishing. [<http://dx.doi.org/10.1063/1.4966655>]

I. INTRODUCTION

Magnetocaloric effect (MCE) is the instinct property of magnetic materials near transition temperature, and the magnetic refrigeration based on MCE has been demonstrated as a promising alternative to the conventional gas compression or expansion refrigeration for its high energy efficiency and environmental friendliness.^{1–5} Lots of efforts have been made to explore the room-temperature MCE materials for the potential application on household refrigerators or air conditioners, and the typical materials with high performance are $\text{Gd}_5\text{Si}_2\text{Ge}_2$,⁶ $\text{La}(\text{Fe},\text{Si})_{13}$,^{7–11} $\text{MnAs}_{1-x}\text{Sb}_x$,¹² $\text{MnFeP}_{1-x}\text{As}_x$,⁴ NiMnSn ,¹³ NiMnIn ,^{14,15} etc. In the past few years, much attention has also been paid on the MCE materials with low transition temperatures such as ErCo_2 ,¹⁶ DyCuAl ,¹⁷ HoCuSi ,¹⁸ TmZn ,¹⁹ ErCr_2Si_2 ,²⁰ ErMn_2Si_2 ,²¹ and RNiBC ($R = \text{Er}, \text{Gd}$)^{22,23} because these materials are promising to be used for gas liquefaction in the magnetic cooling cycle or combined magnetic-gas cooling cycle.^{24,25} The isothermal magnetic entropy change (ΔS_M) and the adiabatic temperature change (ΔT_{ad}) are two important parameters to evaluate MCE materials. Besides exploring new materials with large MCE, much work has also been focused on improving the ΔS_M and ΔT_{ad} of the known MCE materials based on the special physical mechanism.

The binary RNi ($R = \text{Rare earth}$) compounds show interesting magnetic properties, and excellent MCE performance has been observed in some of them. It was found that light-R Nickel compounds crystallize in the CrB-type structure and heavy-R Nickel compounds crystallize in the FeB-type structure.²⁶ YNi and CeNi compounds exhibit Pauli paramagnetism,

while other RNi compounds are all magnetic ordered. Nickel appears to be nonmagnetic in most RNi compounds. A secondary magnetic transition is observed below Curie temperature for NdNi and HoNi compounds.²⁶ Neutron diffraction experiment was employed to study the magnetic structure and magnetic transition of single crystal HoNi compound.²⁷ It was found that the HoNi compound undergoes two magnetic transitions around 15 K and 35 K, respectively. The z component and the x component of the ordered magnetic moment are determined to be antiferromagnetic (AFM) and ferromagnetic (FM), respectively.²⁷ GdNi compound was found to show a collinear magnetic structure, and ErNi compound shows a non-collinear magnetic structure.^{28,29} The MCE of PrNi, GdNi, DyNi, HoNi, and ErNi compounds has been reported.^{30–32} ErNi compound shows one peak on the ΔS_M -T curve with a maximal value of 29.2 J/kg K around 10 K. HoNi compound shows two peaks corresponding to the two magnetic transitions, respectively. The $(\Delta S_M)_{max}$ of ErNi compound is competitive among the MCE materials around 10 K, but there is still some space to be improved.

In this work, the influence of Ho-substitution for Er atoms on the magnetic property and MCE of ErNi compound was studied in detail according to magnetic, heat capacity, and neutron powder diffraction (NPD) measurements. Finally, the results were analyzed and discussed.

II. EXPERIMENTAL DETAILS

Sample fabrication and physical property measurements: Polycrystalline $\text{Ho}_x\text{Er}_{1-x}\text{Ni}$ ($0 \leq x \leq 1$) compounds were prepared by arc melting of Ho, Er, and Ni elements in argon atmosphere, and the molten salts were rotated several times to ensure the homogeneity. The purity of the starting

^{a)}Authors to whom correspondence should be addressed. Electronic addresses: zhengxq@ustb.edu.cn and shenbg@aphy.iphy.ac.cn

elements is more than 99.9%. The annealing and quenching procedure were performed afterwards. Crystal structures of all the samples were determined by powder X-ray diffraction (XRD). Crystal structure and magnetic structures of ErNi, Ho_{0.1}Er_{0.9}Ni, and HoNi compounds at different temperatures were determined by high resolution neutron powder diffraction experiments. Thermal magnetization, ac magnetic susceptibility, and isothermal magnetization curves were measured on the Quantum-designed Vibrating Sample Magnetometer (VSM). Heat capacity data were obtained from the Physical Property Measurement System (PPMS).

Neutron powder diffraction experiments: High resolution neutron powder diffraction data were collected using the BT1 32-detector diffractometer at the NIST Center for Neutron Research (NCNR). A Cu (311) monochromator with the wavelength $\lambda = 1.5403(2)$ Å and in-pile collimation of 60' were used. Data were collected over the 2-theta range of 3°–168° with a step size of 0.05°. A closed cycle refrigerator (CCR) was used in temperature dependent measurements ranging from 3 K to 295 K. The Rietveld refinements were performed using GSAS program.

III. RESULTS AND DISCUSSION

Polycrystalline Ho_xEr_{1-x}Ni ($0 \leq x \leq 1$) compounds were synthesized on the basis of ErNi compound by substituting different contents of Ho for Er atoms. The detailed compositions are ErNi, Ho_{0.05}Er_{0.95}Ni, Ho_{0.1}Er_{0.9}Ni, Ho_{0.2}Er_{0.8}Ni, Ho_{0.3}Er_{0.7}Ni, Ho_{0.4}Er_{0.6}Ni, Ho_{0.6}Er_{0.4}Ni, Ho_{0.8}Er_{0.2}Ni, and HoNi. Powder X-ray diffraction (XRD) experiments were performed for all of the samples, and the results show that Ho_xEr_{1-x}Ni ($0 \leq x \leq 1$) compounds are all pure single phase crystallizing in orthorhombic FeB-type crystal structure (space group No. 62, Pnma). The XRD patterns of Ho_xEr_{1-x}Ni ($0 \leq x \leq 1$) compounds are shown in the [supplementary material](#), Fig. S1. There are four Ho/Er atoms and four Ni atoms in the unit cell, and both Ho/Er and Ni atoms occupy the 4c site (as shown in Fig. S1, [supplementary material](#)). The determined crystal structure is in accord with the reported works.^{31,33}

Zero-field-cooled (ZFC) and field-cooled (FC) magnetization curves were measured under a field of 0.01 T. The FC curves of Ho_xEr_{1-x}Ni ($0 \leq x \leq 1$) compounds are shown in Fig. 1(a). It is found that the Ho-substitution has a large influence on the magnetic transitions of the Ho-Er-Ni compound. Most of the Ho_xEr_{1-x}Ni ($0 \leq x \leq 1$) compounds exhibit two drastic changes on the thermal magnetization curves. The drastic change at higher temperature for each sample is corresponding to a paramagnetic (PM) to ferromagnetic (FM) magnetic transition, and the temperature is known as Curie temperature. As the content of Ho increases, the Curie temperature of Ho_xEr_{1-x}Ni ($0 \leq x \leq 1$) compounds increases monotonically from 11 K to 35.5 K. That is because the Curie temperature is positively correlated with spin (S), and more Ho atoms mean larger average S in Ho_xEr_{1-x}Ni ($0 \leq x \leq 1$) compounds. Most of the Ho_xEr_{1-x}Ni ($0 \leq x \leq 1$) compounds undergo a secondary spin reorientation (SR) transition at a lower temperature besides of the PM to FM transition. The secondary magnetic transition is very

obvious for Ho_xEr_{1-x}Ni ($x = 0.05, 0.3, 0.4, 0.6, 0.8, 1$) compounds. To further investigate the magnetic transition of ErNi, Ho_{0.1}Er_{0.9}Ni, and Ho_{0.2}Er_{0.8}Ni compounds, the ZFC and FC curves together with the derivation of FC for $x = 0, 0.1, \text{ and } 0.2$ compositions are shown in Figs. 1(b), 1(c), and 1(d), respectively. For ErNi compound, the dM/dT curve shows a minimal value at $T_{SR} \sim 7$ K and $T_C \sim 11$ K, respectively. It indicates that the ErNi compound undergoes two magnetic transitions as the temperature increases. The secondary magnetic transition at 7 K is inconspicuous, but it can be observed from the dM/dT curve. Actually, the SR transition of ErNi has been detected on the M-T curve by Kumar *et al.*, though it is not mentioned.³¹ For Ho_{0.2}Er_{0.8}Ni compound, the secondary magnetic transition is more inconspicuous. It cannot be observed from the dM/dT curve, but can be observed from the ZFC curve. The T_{SR} and T_C are determined to be 6 K and 13.5 K, respectively. For Ho_{0.1}Er_{0.9}Ni compound, the minimal value of dM/dT was observed at $T_C \sim 11$ K only and FC curve begins to decrease with the temperature decreasing around 9 K corresponding to SR transition (see Fig. 1(c)). To further understand the magnetization behavior with temperature changing, ac magnetic susceptibility measurements, in response to a 5 Oe, 97 Hz driving field, were performed for ErNi and Ho_{0.1}Er_{0.9}Ni compounds as shown in Figs. 1(e) and 1(f), respectively. The ac magnetic susceptibility measurements are usually used to investigate the SR transition and FM to PM transition.^{34,35} In some cases, both SR transition and FM to PM transition show an obvious change on the real (χ') and imaginary (χ'') parts of ac magnetic susceptibility.^{34,35} But in some other cases, SR transition or FM to PM transition shows an obvious change on χ' or χ'' only.³⁴ According to the results as shown in Figs. 1(e) and 1(f), for ErNi and Ho_{0.1}Er_{0.9}Ni compounds, only the χ' shows an obvious response to FM to PM transition and only the χ'' shows an obvious response to SR transition. The SR transition and FM to PM transition occur around 7 K and 11 K, respectively, for ErNi compound, showing a consistent result with dc measurements. The transition temperatures determined from the ac magnetic susceptibility are in accord with those determined from dc measurement for Ho_{0.1}Er_{0.9}Ni compound, too. All of the transition temperatures of Ho_xEr_{1-x}Ni ($0 \leq x \leq 1$) compounds are listed in Table I. It can be seen that 10% of Ho-substitution for Er atoms obviously shortens the temperature interval between SR transition and FM to PM transition.

In order to investigate the magnetic structure and the evolution of magnetic structure as the temperature changes, high resolution neutron powder diffraction (NPD) experiments were employed at different temperatures for ErNi, Ho_{0.1}Er_{0.9}Ni, and HoNi compounds. For magnetic materials, only nuclear-based crystal structure contributes to the NPD patterns in the PM temperature zone, but both nuclear and magnetic structures show contributions in the magnetic ordered temperature zone. Compared with the patterns at high temperature above T_C , there are some additional or significantly enhanced peaks at low temperature, which are supposed to be magnetic signals. The magnetic transitions can be analyzed from the change of magnetic peaks as the temperature increases. The temperature dependence of the

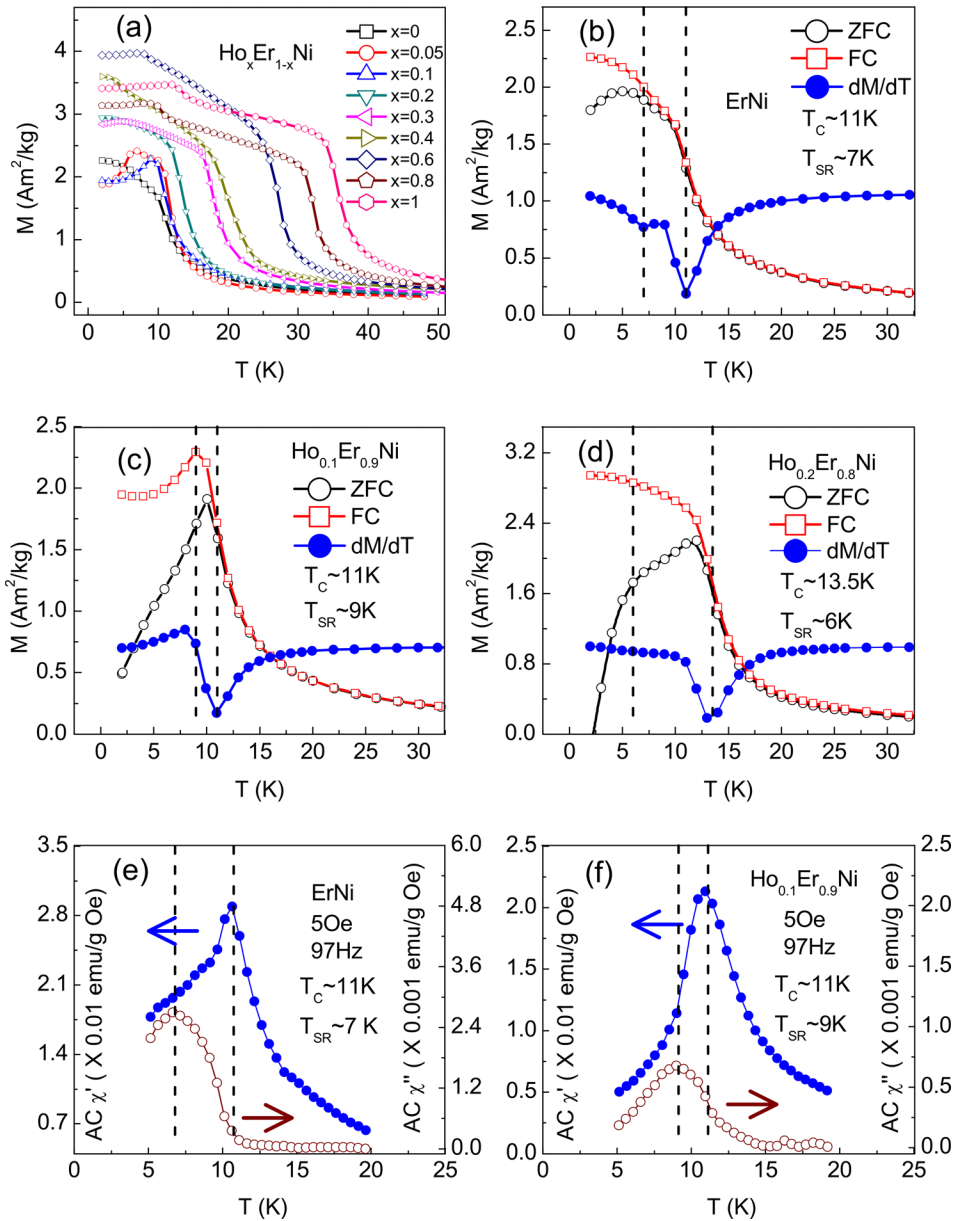


FIG. 1. (a) The field-cooled magnetization curves under a field of 0.01 T for $\text{Ho}_x\text{Er}_{1-x}\text{Ni}$ ($0 \leq x \leq 1$) compounds. The zero-field-cooled, field-cooled, and first-order differentiation of FC curves for ErNi (b), $\text{Ho}_{0.1}\text{Er}_{0.9}\text{Ni}$ (c), and $\text{Ho}_{0.2}\text{Er}_{0.8}\text{Ni}$ (d). The temperature dependence of ac susceptibility in response to a 5 Oe, 97 Hz driving field for ErNi (e) and $\text{Ho}_{0.1}\text{Er}_{0.9}\text{Ni}$ (f).

intensities of typical magnetic peaks for ErNi and $\text{Ho}_{0.1}\text{Er}_{0.9}\text{Ni}$ compounds is shown in Figs. 2(a) and 2(b), respectively. It can be seen that the temperature zone where the magnetic peak changes rapidly for the ErNi compound

TABLE I. The transition temperatures, maximum value of magnetic entropy changes, refrigerant temperature changes, and refrigerant capacities for $\text{Ho}_x\text{Er}_{1-x}\text{Ni}$ ($0 \leq x \leq 1$) compounds for a field change of 5 T.

Materials	T_{SR} (K)	T_{C} (K)	$-\Delta S_{\text{M}}(T)_{\text{max}}$ (J/kg K)	δT_{FWHM} (K)	RC (J/kg)
ErNi	7.0	11.0	29.6	15.6	350.0
$\text{Ho}_{0.05}\text{Er}_{0.95}\text{Ni}$	7.0	11.5	32.3	15.1	364.7
$\text{Ho}_{0.1}\text{Er}_{0.9}\text{Ni}$	9.0	11.0	34.0	14.2	366.6
$\text{Ho}_{0.2}\text{Er}_{0.8}\text{Ni}$	6.0	13.5	28.3	18.2	392.3
$\text{Ho}_{0.3}\text{Er}_{0.7}\text{Ni}$	5.0	16.5	25.3	21.3	407.7
$\text{Ho}_{0.4}\text{Er}_{0.6}\text{Ni}$	4.0	20.0	20.7	26.3	418.0
$\text{Ho}_{0.6}\text{Er}_{0.4}\text{Ni}$	9.0	27.0	16.1	34.2	431.1
$\text{Ho}_{0.8}\text{Er}_{0.2}\text{Ni}$	11.0	32.0	16.1	40.1	487.3
HoNi	13.5	35.5	16.6	41.6	556.7

can be divided into two stages, which correspond to the SR transition and the FM to PM transition, respectively. But for the $\text{Ho}_{0.1}\text{Er}_{0.9}\text{Ni}$ compound, only FM to PM transition can be observed from the signals of (110) peak. That is probably because the SR transition is so close to FM to PM transition that SR transition temperature cannot be separated from the Curie temperature.

The NPD experiments were performed at different temperatures for ErNi, $\text{Ho}_{0.1}\text{Er}_{0.9}\text{Ni}$, and HoNi compounds. Fitting and calculations were done based on the Rietveld refinement method. The observed and calculated NPD patterns at room temperature and low temperature for ErNi, $\text{Ho}_{0.1}\text{Er}_{0.9}\text{Ni}$, and HoNi are shown in supplementary Figs. S2, S3, and S4, respectively. According to the data obtained at 295 K, three compounds are all pure phase, and the resolved crystal structure is in accord with those obtained from XRD experiments. The resolved crystal structure and the magnetic structure at 3 K for ErNi compound are shown in Fig. 2(c), and the four Er atoms in the unit cell are marked as #1—#4. The Er atoms connect in the form of hexagon

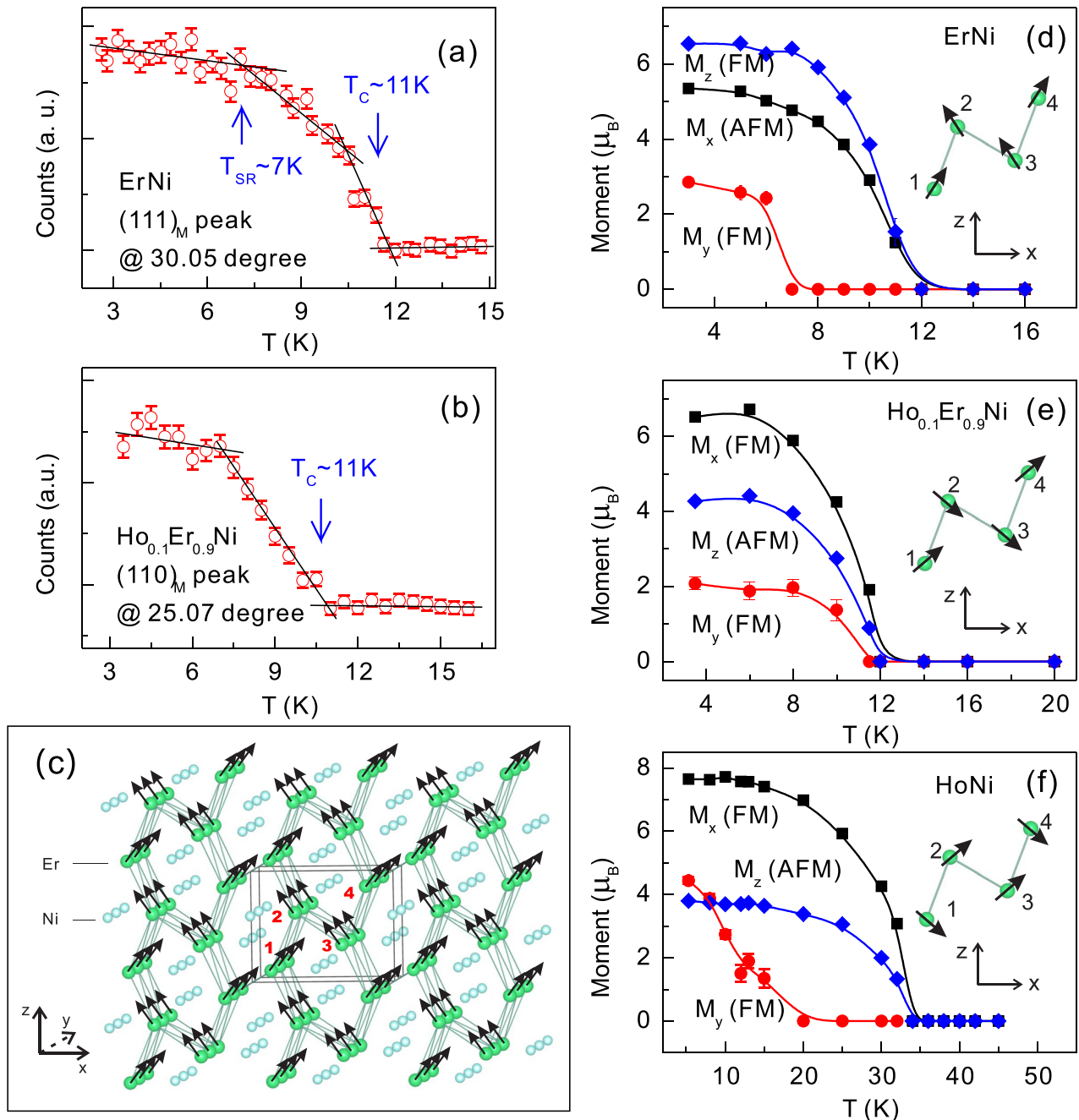


FIG. 2. The temperature dependence of typical magnetic peaks for ErNi (a) and $\text{Ho}_{0.1}\text{Er}_{0.9}\text{Ni}$ (b) compounds. (c) The magnetic structure at 3 K for ErNi compound. The four Er atoms in the unit cell are marked from #1 to #4. The evolution of the magnetic structure as the temperature increases for ErNi (d), $\text{Ho}_{0.1}\text{Er}_{0.9}\text{Ni}$ (e), and HoNi (f) compounds.

rings and the Ni atoms are within the rings. The four Er atoms in every unit cell group in a parallelogram, and they are divided into two groups. The #1 and #4 atoms are FM ordered with a positive x component ($5.35 \mu_B$) and a positive z component ($6.54 \mu_B$). The #2 and #3 atoms are also FM ordered but with a negative x component and a positive z component. Besides, there is an FM ordered y component as well with the value of $2.9 \mu_B$, which cannot be presented in Fig. 2(c). From the full view, FM order and AFM order coexist in ErNi at 3 K.

The magnetic structures were determined at different temperatures, and the detailed data for ErNi, $\text{Ho}_{0.1}\text{Er}_{0.9}\text{Ni}$, and HoNi are shown in supplementary Tables S5(a), S5(b),

S6(a), S6(b), S7(a), S7(b), and S7(c), respectively. The evolutions of magnetic structures for ErNi, $\text{Ho}_{0.1}\text{Er}_{0.9}\text{Ni}$, and HoNi compounds with temperature increasing are shown in Figs. 2(d), 2(e), and 2(f), respectively. As mentioned above, the ordered magnetic moment includes an AFM x component (M_x), an FM y component (M_y), and an FM z component (M_z) at 3 K for ErNi compound. As the temperature increases, the FM ordered M_y disappears at $T \sim 7\text{K}$, but the M_x and M_z do not decrease to zero until $T \sim 11\text{K}$. The temperature where M_y disappears corresponds to T_{SR} , and the temperature where M_x and M_z disappear corresponds to T_c . As for $\text{Ho}_{0.1}\text{Er}_{0.9}\text{Ni}$ compound, the type of magnetic coupling at low temperatures for M_x , M_y , and M_z is FM, FM,

and AFM order, respectively, which is the same as the ErNi compound. M_x , M_y , and M_z decrease to zero at the similar temperature around 11 K which is supposed to be Curie temperature. The existence of SR transition has been confirmed by the magnetic measurement, but it is not observed here because the two transitions are too close and the intensity of NPD pattern is not high enough. As for HoNi compound, the FM ordered M_y disappears around 13.5 K and the FM ordered M_x along with AFM ordered M_z vanishes around 35.5 K. The two transition temperatures correspond to SR transition and order to disorder transition, respectively. The general situation of HoNi compound is similar to ErNi, but the coupling type of M_x and M_z is opposite. The result of HoNi is in accord with previous works by Sato *et al.*³³ It should also be noted that although the magnetic order of M_x and M_z for HoNi and $\text{Ho}_{0.1}\text{Er}_{0.9}\text{Ni}$ compounds is the same, the specific directions of every magnetic atom are different (see the inset of Figs. 2(e) and 2(f)). In addition, the FM order and AFM order coexist in all three compounds; hence, they should be called as canted magnetic materials. For simplification, the order to disorder magnetic transition is still described as FM to PM transition. It can be concluded that ErNi and HoNi compounds both undergo two magnetic transitions, but the SR transition becomes indistinct for $\text{Ho}_{0.1}\text{Er}_{0.9}\text{Ni}$ compound because it is very close to FM to PM transition.

The isothermal magnetization curves at different temperatures were measured, and the ΔS_M was calculated for all of the $\text{Ho}_x\text{Er}_{1-x}\text{Ni}$ ($0 \leq x \leq 1$) compounds by using Maxwell relation $\Delta S_M = \int_0^H (\partial M / \partial T)_H dH$.⁶ The temperature dependence of ΔS_M for a field change of 0–5 T is shown in Fig. 3(a), and the enlarged view of ΔS_M -T curves for ErNi, $\text{Ho}_{0.05}\text{Er}_{0.95}\text{Ni}$, $\text{Ho}_{0.1}\text{Er}_{0.9}\text{Ni}$, and $\text{Ho}_{0.2}\text{Er}_{0.8}\text{Ni}$ compounds is shown in Fig. 3(b). It is found that the $(\Delta S_M)_{\max}$ of $\text{Ho}_{0.1}\text{Er}_{0.9}\text{Ni}$ is the largest among $\text{Ho}_x\text{Er}_{1-x}\text{Ni}$ ($0 \leq x \leq 1$) compounds. The value of $(\Delta S_M)_{\max}$ for ErNi and $\text{Ho}_{0.1}\text{Er}_{0.9}\text{Ni}$ compound is 29.6 J/kg K

and 34 J/kg K, respectively; i.e., 10% of Ho-substitution brings as high as $\sim 14.9\%$ $((34-29.6)/29.6 = 0.149)$ enhancement on $(\Delta S_M)_{\max}$. Adiabatic temperature change (ΔT_{ad}) is another important parameter to evaluate MCE materials. The temperature dependences of heat capacity were measured at zero field for ErNi, $\text{Ho}_{0.1}\text{Er}_{0.9}\text{Ni}$, and $\text{Ho}_{0.2}\text{Er}_{0.8}\text{Ni}$ compounds. Then, ΔT_{ad} were calculated by using the method proposed by Pecharsky and Gschneidner.³⁶ The temperature dependence of ΔT_{ad} curves for ErNi, $\text{Ho}_{0.1}\text{Er}_{0.9}\text{Ni}$, and HoNi compounds is shown in Fig. 3(c). The peak values are determined to be 7.3 K, 8.9 K, and 8.0 K for ErNi, $\text{Ho}_{0.1}\text{Er}_{0.9}\text{Ni}$, and $\text{Ho}_{0.2}\text{Er}_{0.8}\text{Ni}$ compounds, respectively. It can be clearly seen that $\text{Ho}_{0.1}\text{Er}_{0.9}\text{Ni}$ compound shows the best performance on ΔT_{ad} ; i.e., its maximum value of ΔT_{ad} shows an enhancement of $\sim 21.9\%$ $((8.9-7.3)/7.3 = 0.219)$ compared to the ErNi compound. The refrigerant capacity (RC) of $\text{Ho}_x\text{Er}_{1-x}\text{Ni}$ ($0 \leq x \leq 1$) compounds was also calculated by using the approach suggested by Gschneidner *et al.*³⁷ The RC is defined as $RC = \int_{T_1}^{T_2} |\Delta S_M| dT$, where T_1 and T_2 are the temperatures corresponding to both sides of the half-maximum value of $(\Delta S_M)_{\max}$, respectively. The refrigerant temperature width (δT_{FWHM}) is defined as the temperature span of the full width at half maximum value of $(\Delta S_M)_{\max}$. Then, (δT_{FWHM}) can be obtained by $T_2 - T_1$.

All the MCE parameters, including $(\Delta S_M)_{\max}$, δT_{FWHM} , and RC for a field change of 0–5 T for $\text{Ho}_x\text{Er}_{1-x}\text{Ni}$ ($0 \leq x \leq 1$) compounds, are listed in Table I, and Ho-content dependences of the above three parameters are plotted in Fig. 3(d). As the content of Ho increases, the $(\Delta S_M)_{\max}$ first increases and then decreases. Among all the $\text{Ho}_x\text{Er}_{1-x}\text{Ni}$ ($0 \leq x \leq 1$) compounds, $\text{Ho}_{0.1}\text{Er}_{0.9}\text{Ni}$ compound shows the largest $(\Delta S_M)_{\max}$. $\text{Ho}_{0.1}\text{Er}_{0.9}\text{Ni}$ compound has proved to be a second-order-transition material according to Arrott plots, but the $(\Delta S_M)_{\max}$ (34 J/kg K for 0–5 T) is comparable to the representative low temperature first-order-transition MCE material ErCo_2 compound (36.8 J/kg K for 0–5 T).³⁸ The

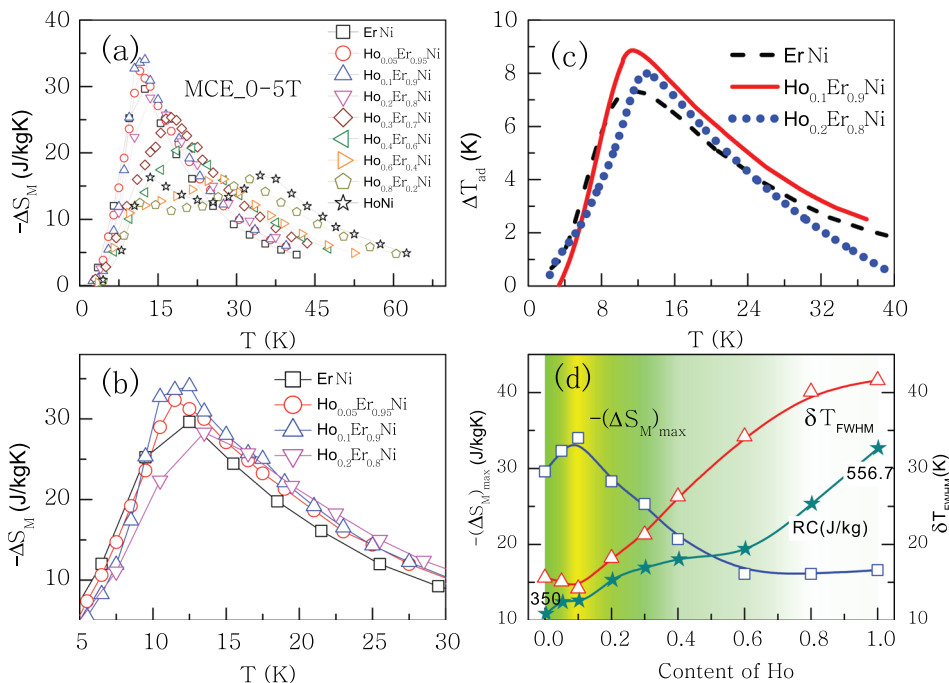


FIG. 3. (a) The temperature dependence of magnetic entropy change for a field change of 0–5 T for $\text{Ho}_x\text{Er}_{1-x}\text{Ni}$ ($0 \leq x \leq 1$) compounds. (b) The enlarged view of magnetic entropy change curves for ErNi, $\text{Ho}_{0.05}\text{Er}_{0.95}\text{Ni}$, $\text{Ho}_{0.1}\text{Er}_{0.9}\text{Ni}$, and $\text{Ho}_{0.2}\text{Er}_{0.8}\text{Ni}$ compounds. (c) The adiabatic temperature change curves for a field change of 0–5 T for ErNi, $\text{Ho}_{0.1}\text{Er}_{0.9}\text{Ni}$, and $\text{Ho}_{0.2}\text{Er}_{0.8}\text{Ni}$ compounds. (d) The maximal magnetic entropy change, the refrigerant temperature width, and the refrigerant capacity versus Ho-content curves.

changing trend of δT_{FWHM} is opposite to $(\Delta S_{\text{M}})_{\text{max}}$. Among all the $\text{Ho}_x\text{Er}_{1-x}\text{Ni}$ ($0 \leq x \leq 1$) compounds, $\text{Ho}_{0.1}\text{Er}_{0.9}\text{Ni}$ compound shows the smallest δT_{FWHM} . As for RC, it increases monotonously from 350 J/kg to 556.7 J/kg as the content of Ho changes from 0 to 1. Since the value of RC is improper when ΔT_{ad} is far smaller than δT_{FWHM} , RC is acceptable, considering that ΔT_{ad} is comparable to δT_{FWHM} in order of magnitude for ErNi, $\text{Ho}_{0.1}\text{Er}_{0.9}\text{Ni}$, and $\text{Ho}_{0.2}\text{Er}_{0.8}\text{Ni}$ compounds. For Ho-Er-Ni compounds, $\text{Ho}_{0.1}\text{Er}_{0.9}\text{Ni}$ exerts ideal $(\Delta S_{\text{M}})_{\text{max}}$ but with ordinary δT_{FWHM} and RC. But, it is valuable to discuss the MCE enhancement (peak value) with 10% of Ho-substitution compared with ErNi.

In fact, the MCE enhancement in Ho-Er-Ni compounds is closely related to the temperature interval between SR transition and FM to PM transition. Magnetic materials are in the non-steady magnetic state around transition temperatures. When a field is applied around the transition temperature, obvious MCE can be observed because the magnetic entropy is easy to change in this state. As a result, more than one ΔS_{M} peaks can be observed in multi-phase-transition MCE materials, such as ErGa³⁹ and Ho₂In⁴⁰ compounds. According to thermal magnetization and ac susceptibility measurements, all of the $\text{Ho}_x\text{Er}_{1-x}\text{Ni}$ ($0 \leq x \leq 1$) compounds undergo two magnetic transitions as the temperature increases: SR transition and FM to PM transition. More specially, the temperature interval between the two transitions is only 2 K for $\text{Ho}_{0.1}\text{Er}_{0.9}\text{Ni}$, which is the smallest value among the $\text{Ho}_x\text{Er}_{1-x}\text{Ni}$ ($0 \leq x \leq 1$) compounds. Though NPD experiments cannot detect the SR transition in the $\text{Ho}_{0.1}\text{Er}_{0.9}\text{Ni}$ compound, the results support the conclusion that the SR transition and FM to PM transition are very close to each other. When the temperature interval between the magnetic transitions is large, the corresponding two ΔS_{M} peaks are separate, such as HoNi, $\text{Ho}_{0.8}\text{Er}_{0.2}\text{Ni}$, and $\text{Ho}_{0.6}\text{Er}_{0.4}\text{Ni}$ compounds (see Fig. 3(a)). But for other samples, the two peaks are hard to distinguish, because they overlap and merge together, which is similar to $\text{Ho}_{12}\text{Co}_7$ compound with a large field change.⁴¹ In this case, δT_{FWHM} can also be used to evaluate the level of overlap. It is conspicuous that the δT_{FWHM} is the smallest for $\text{Ho}_{0.1}\text{Er}_{0.9}\text{Ni}$ compound, indicating that the two ΔS_{M} peaks are almost entire-overlapping. Therefore, $\text{Ho}_{0.1}\text{Er}_{0.9}\text{Ni}$ compound shows the largest $(\Delta S_{\text{M}})_{\text{max}}$ and the largest $(\Delta T_{\text{ad}})_{\text{max}}$.

IV. CONCLUSION

The existence of SR transition was confirmed by magnetic measurements and NPD experiments for $\text{Ho}_x\text{Er}_{1-x}\text{Ni}$ ($0 \leq x \leq 1$) compounds. The temperature interval between SR transition and FM to PM transition is the smallest for $\text{Ho}_{0.1}\text{Er}_{0.9}\text{Ni}$ compound. As a result, $\text{Ho}_{0.1}\text{Er}_{0.9}\text{Ni}$ compound shows the largest $(\Delta S_{\text{M}})_{\text{max}}$ and $(\Delta T_{\text{ad}})_{\text{max}}$ among the $\text{Ho}_x\text{Er}_{1-x}\text{Ni}$ ($0 \leq x \leq 1$) compounds. Compared with ErNi compound, 10% of the Ho-substitution gives $\sim 14.9\%$ of enhancement in $(\Delta S_{\text{M}})_{\text{max}}$ and $\sim 21.9\%$ of enhancement in $(\Delta T_{\text{ad}})_{\text{max}}$. The MCE enhancement based on the atom substitution may be instructive for designing high-performance magnetic functional materials.

SUPPLEMENTARY MATERIAL

See [supplementary material](#) for the XRD patterns and NPD data of the $\text{Ho}_x\text{Er}_{1-x}\text{Ni}$ ($0 \leq x \leq 1$) compounds.

ACKNOWLEDGMENTS

This work was supported by the National Basic Research Program of China (973 program, Grant No. 2014CB643700), the National Natural Science Foundation of China (Grant Nos. 51501005, 11274357, 51531008, and 51271196), the Fundamental Research Funds for the Central Universities (Grant No. FRF-TP-15-010A1), China Postdoctoral Science Foundation funded project (Grant No. 2016M591071), the Strategic Priority Research Program B (Grant No. XDB07030200), and the Key Research Program of the Chinese Academy of Sciences.

- ¹E. Brück, *J. Phys. D: Appl. Phys.* **38**, R381 (2005).
- ²V. K. Pecharsky and K. A. Gschneidner, Jr., *J. Magn. Magn. Mater.* **200**, 44 (1999).
- ³K. A. Gschneidner, Jr. and V. K. Pecharsky, *Annu. Rev. Mater. Sci.* **30**, 387 (2000).
- ⁴O. Tegus, E. Brück, K. H. J. Buschow, and F. R. de Boer, *Nature* **415**, 150 (2002).
- ⁵J. Glanz, *Science* **279**, 2045 (1998).
- ⁶V. K. Pecharsky and K. A. Gschneidner, *Phys. Rev. Lett.* **78**, 4494 (1997).
- ⁷F. X. Hu, B. G. Shen, J. R. Sun, Z. H. Cheng, G. H. Rao, and X. X. Zhang, *Appl. Phys. Lett.* **78**, 3675 (2001).
- ⁸F. X. Hu, B. G. Shen, J. R. Sun, and X. X. Zhang, *Chin. Phys.* **9**, 550 (2000).
- ⁹F. W. Wang, X. X. Zhang, and F. X. Hu, *Appl. Phys. Lett.* **77**, 1360 (2000).
- ¹⁰X. X. Zhang, G. H. Wen, F. W. Wang, W. H. Wang, C. H. Yu, and G. H. Wu, *Appl. Phys. Lett.* **77**, 3072 (2000).
- ¹¹X. X. Zhang, F. W. Wang, and G. H. Wen, *J. Phys.: Condens. Matter* **13**, L747 (2001).
- ¹²H. Wada and Y. Tanabe, *Appl. Phys. Lett.* **79**, 3302 (2001).
- ¹³T. Krenke, E. Duman, M. Acet, E. F. Wassermann, X. Moya, L. Mañosa, and A. Planes, *Nat. Mater.* **4**, 450 (2005).
- ¹⁴Z. D. Han, D. H. Wang, C. L. Zhang, S. L. Tang, B. X. Gu, and Y. W. Du, *Appl. Phys. Lett.* **89**, 182507 (2006).
- ¹⁵J. Liu, T. Gottschall, K. P. Skokov, J. D. Moore, and O. Gutfleisch, *Nat. Mater.* **11**, 620 (2012).
- ¹⁶A. Giguere, M. Foldeaki, W. Schnelle, and E. Gmelin, *J. Phys.: Condens. Matter* **11**, 6969 (1999).
- ¹⁷Q. Y. Dong, B. G. Shen, J. Chen, J. Shen, and J. R. Sun, *J. Appl. Phys.* **105**, 113902 (2009).
- ¹⁸J. Chen, B. G. Shen, Q. Y. Dong, F. X. Hu, and J. R. Sun, *Appl. Phys. Lett.* **96**, 152501 (2010).
- ¹⁹L. Li, Y. Yuan, Y. Zhang, T. Namiki, K. Nishimura, R. Pöttgen, and S. Zhou, *Appl. Phys. Lett.* **107**, 132401 (2015).
- ²⁰L. Li, W. D. Hutchison, D. Huo, T. Namiki, Z. Qian, and K. Nishimura, *Scr. Mater.* **67**, 237 (2012).
- ²¹L. Li, K. Nishimura, W. D. Hutchison, Z. Qian, D. Huo, and T. NamiKi, *Appl. Phys. Lett.* **100**, 152403 (2012).
- ²²L. Li, M. Kadonaga, D. Huo, Z. Qian, T. Namiki, and K. Nishimura, *Appl. Phys. Lett.* **101**, 122401 (2012).
- ²³L. W. Li, *Chin. Phys. B* **25**, 037502 (2016).
- ²⁴H. Yayama, Y. Hatta, Y. Makimoto, and A. Tomokiyo, *Jpn. J. Appl. Phys., Part 1* **39**, 4220 (2000).
- ²⁵K. A. Gschneidner, Jr., V. K. Pecharsky, and A. O. Tsokol, *Rep. Prog. Phys.* **68**, 1479 (2005).
- ²⁶R. E. Walline and W. E. Wallace, *J. Chem. Phys.* **41**, 1587 (1964).
- ²⁷Y. Isikawa, K. Mori, K. Sato, M. Ohashi, and Y. Yamaguchi, *J. Appl. Phys.* **55**, 2031 (1984).
- ²⁸S. C. Abrahams, J. L. Bernstein, R. C. Sherwood, J. H. Wernick, and H. J. Williams, *J. Phys. Chem. Solids* **25**, 1069 (1964).
- ²⁹D. Gignoux, *J. Phys.* **35**, 455 (1974).
- ³⁰S. K. Tripathy, K. G. Suresh, R. Nirmala, A. K. Nigam, and S. K. Malik, *Solid State Commun.* **134**, 323 (2005).

- ³¹P. Kumar, K. G. Suresh, A. K. Nigam, and O. Gutfleisch, *J. Phys. D: Appl. Phys.* **41**, 245006 (2008).
- ³²A. Pecharsky, Y. Mozharivskyj, K. Dennis, K. Gschneidner, R. McCallum, G. Miller, and V. Pecharsky, *Phys. Rev. B* **68**, 134452 (2003).
- ³³K. Sato, S. Iwasaki, Y. Ishikawa, and K. Mori, *J. Appl. Phys.* **53**, 1938 (1982).
- ³⁴K. Y. Wang, M. Sawicki, K. Edmonds, R. Campion, S. Maat, C. Foxon, B. Gallagher, and T. Dietl, *Phys. Rev. Lett.* **95**, 217204 (2005).
- ³⁵Y. Liu, L. Peng, J. Zhang, Z. Ren, J. Yang, Z. Yang, S. Cao, and W. Fang, *Europhys. Lett.* **96**, 27015 (2011).
- ³⁶V. K. Pecharsky and K. A. Gschneidner, *J. Appl. Phys.* **86**, 565 (1999).
- ³⁷K. A. Gschneidner, Jr., V. K. Pecharsky, A. O. Pecharsky, and C. B. Zimm, *Mater. Sci. Forum* **315–317**, 69 (1999).
- ³⁸H. Wada, Y. Tanabe, M. Shiga, H. Sugawara, and H. Sato, *J. Alloys Compd.* **316**, 245 (2001).
- ³⁹J. Chen, B. G. Shen, Q. Y. Dong, F. X. Hu, and J. R. Sun, *Appl. Phys. Lett.* **95**, 132504 (2009).
- ⁴⁰Q. Zhang, J. H. Cho, B. Li, W. J. Hu, and Z. D. Zhang, *Appl. Phys. Lett.* **94**, 182501 (2009).
- ⁴¹X. Q. Zheng, X. P. Shao, J. Chen, Z. Y. Xu, F. X. Hu, J. R. Sun, and B. G. Shen, *Appl. Phys. Lett.* **102**, 022421 (2013).